Validation of Neutron Flux and Activation in the Nagra AMAC model of the Mühleberg Power Plant

Valentyn Bykov[1,*], *Ben* Volmert[1], *Sylvain* Pelloux[2], and *Erwin* Neukäter[2]

[1] Nagra (National Cooperative for the Disposal of Radioactive Waste), Hardstrasse 73, 5430 Wettingen, Switzerland
[2] BKW Energie, Kernkraftwerk Mühleberg, 3203 Mühleberg, Switzerland

Abstract. The decommissioning of the Mühleberg Nuclear Power Plant (KKM) is supported by Nagra (National Cooperative for the Disposal of Radioactive Waste) through computational analysis of neutron activation in the reactor components and structures using the Nagra Advanced Methodology for Activation Characterization (AMAC). To validate these calculations, measurements of neutron flux and neutron-induced activity were carried out in the form of two foil activation campaigns (72 samples) and three concrete sampling campaigns (118 samples). Generally, the ratio of calculated to measured activities is in the order of 2 in the proximity of the reactor pressure vessel and 3 in the upper sections of the drywell. As expected, the flux in the lower (spherical) part of the drywell is significantly overestimated due to the simplified modelling of this space. The overestimation, which ratios of up to 10, can be corrected by scaling the calculated radionuclide activity distributions in the vicinity of the validation locations.

1 Introduction

The Mühleberg Power Plant (KKM) is a General Electric Type-4 boiling water reactor (BWR/4) with Mark I containment, located in Switzerland. KKM was shutdown on December 20, 2019 and is presently being decommissioned. Nagra, the Swiss national cooperative for the disposal of radioactive waste, is supporting this project by applying its Advanced Methodology for Activation Characterization (AMAC) to characterize the neutron activation within the reactor internals, the reactor pressure vessel (RPV), and the surrounding structures. This work represents the first look at the comprehensive results of the measurement campaigns carried out to validate the neutron flux and activation calculated with AMAC.

* Corresponding author: valentyn.bykov@nagra.ch

2 Nagra Advanced Methodology for Activation Characterization (AMAC)

In order to quantify the amount of radioactive waste arising from nuclear power plant decommissioning, Nagra utilizes AMAC [1], based on three-dimensional MCNP [2] models of the plant.

Inside the RPV, the geometry is well known. The structures are typically well documented and only rarely change during the lifetime of the plant. Conversely, outside of the RPV, the information is much scarcer. There are generally no records of the objects filling the surrounding room over the lifetime of a plant, let alone their exact dimensions, weight, and material compositions. Many of the objects also tend to be moved, added, or removed. This poses a challenge for the accurate modeling of neutron transport in the plant.

Filling the room with a homogenized mixture of a typically expected amount of material (representing the objects inside the room) has been observed to lead to an incorrect neutron spectrum and overestimation of shielding provided by the objects. This is due to the fact that in reality, neutrons can pass in between the various objects (which occupy only a fraction of the space inside the room). Conversely, when a homogenized mixture fills the room, all neutrons are guaranteed to encounter (albeit diluted) shielding material. For this reason, a conservative assumption is made for all MCNP models used for AMAC: rooms are assumed to be empty. This unavoidably leads to an overestimation of the neutron flux (due to the absence of any shielding materials along the neutron path in these rooms). However, this conservative assumption is deemed preferential to an underestimation of the neutron flux. Figure 1 shows the MCNP model of KKM; it can be seen that the drywell is modeled as empty.

The effect of this overestimation typically grows with distance from the neutron source, as more and more shielding material is neglected along the path in those empty rooms. Therefore, a comparison of calculated quantities against measurements is highly desirable, as it allows the determination of the degree of flux overestimation in the area. Since the AMAC modeling of the power plants also involves other assumptions and simplifications, it is also desirable to validate the quantities calculated for the structures close to the core (where the empty room assumption isn't the leading source of error).

Validation of AMAC calculations has typically been achieved in two ways. The first approach, typically done when the power plant is still operating, validates the neutron flux using in-situ foil activation. The second approach, mostly done following the final shutdown of the plant, validates the activity of the neutron activation induced radionuclides within plant components and structures against measurements.

3 Flux Validation with Activation Foils

Neutron transport is validated by in-situ sample activation campaigns, in which small metal foils, stacked inside cylindrical containers, are placed at key locations during a refueling outage and removed during the subsequent outage, thereby being activated during one whole reactor cycle. The activity of activation products is measured with gamma spectrometry and compared with the values calculated using the MCNP model.

Two separate foil-activation campaigns have been carried out at KKM. The first campaign took place during reactor cycle 33 (2005-2006) and involved 50 samples, including two chains of 18 and 14 samples, respectively, installed on the inner and outer surface of the bioshield. The second campaign took place during reactor cycle 39 (2012-2013) and involved 22 samples. The locations of all these samples are summarized in Figure 1.

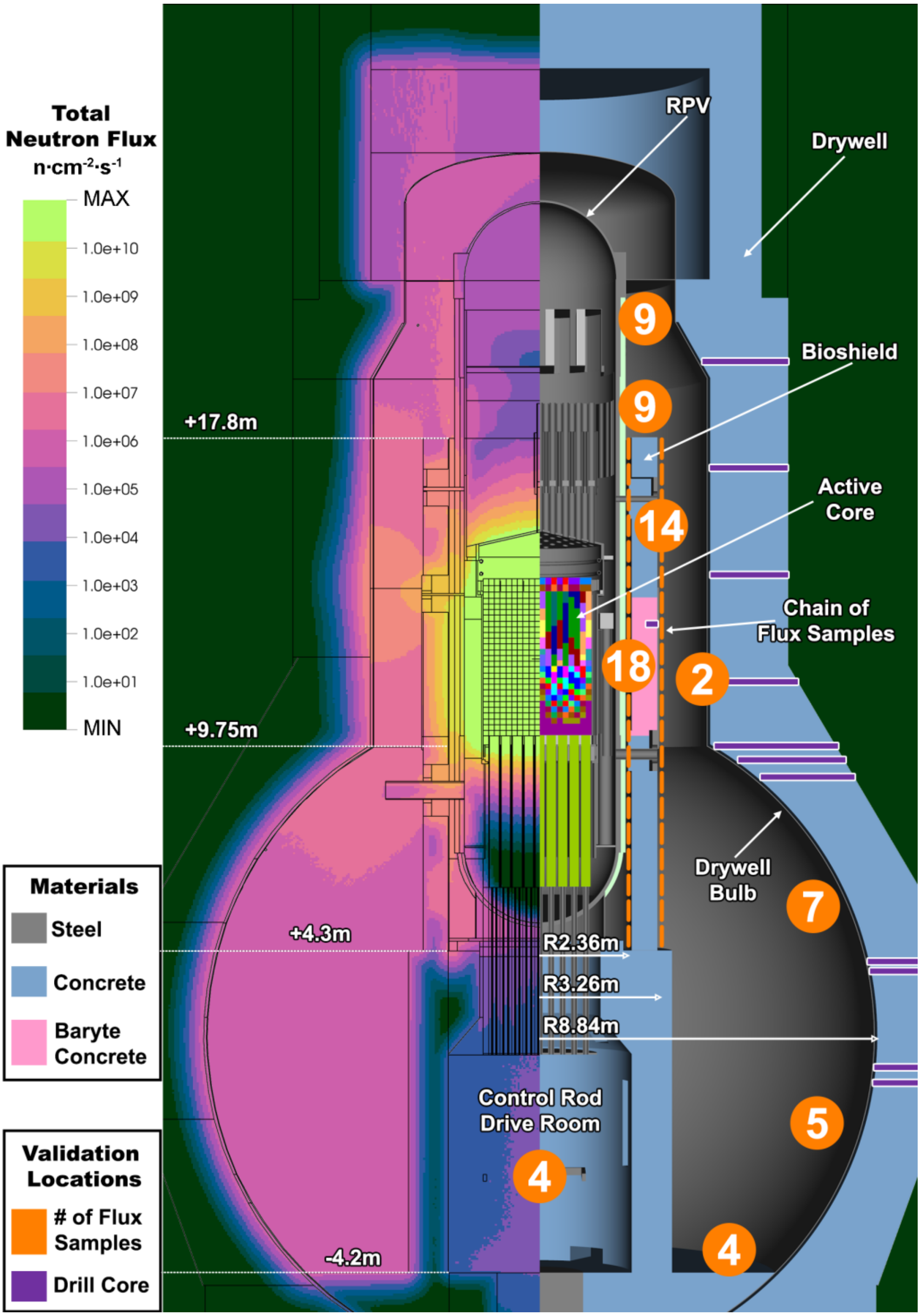

Figure 1. MCNP model of KKM, showing the total neutron flux distribution (left) and the modeled geometry (right), including a summary of the locations of the flux samples and the drill cores. The geometry is color-coded based on the material type. The number of flux samples in a particular area are indicated within orange circles. The locations of drill cores are indicated using purple rectangles. Key dimensions are provided as orientation for the sample positions defined in subsequent tables.

3.1 Methodology

The foil material is chosen based on the following three criteria. Since the sample is activated for one reactor cycle (in Switzerland typically approximately one year long), the chosen materials must have activation products with sufficiently long half-lives. Furthermore, the activation products need to be easily detectable, preferably with gamma spectrometry. Finally, the chosen foil materials should provide information about the energy distribution of the neutron flux. Based on these criteria, cobalt, silver, and nickel were chosen for AMAC validation. In subsequent validation campaigns, scandium was added to provide additional information about the epi-thermal energy range. Figure 2 shows the relevant cross sections, as well as an extruded cut view of a validation sample (foils inside an aluminum capsule). For both ^{59}Co and ^{109}Ag the majority of activation happens at the energy of the first peak (131 eV for ^{59}Co and 5.22 eV for ^{109}Ag, respectively). ^{58}Ni activation has a threshold of approximately 500 keV and majority of reactions occurring at even higher energies. As such, ^{58}Ni activation is representative of the fast neutron flux.

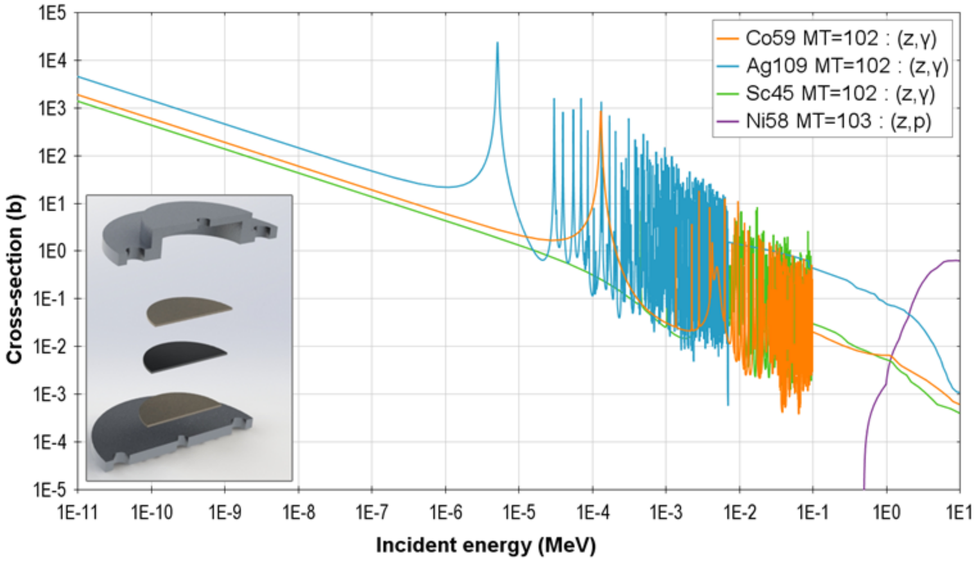

Figure 2. Cross sections of relevant foil activation reactions; bottom left: extruded cut view of a validation sample (foils inside a capsule).

The foil thickness is selected based on the expected neutron fluence (based on the past measurements and modeling experience with other plants), such that the activity of the resulting activation products is high enough for the spectrometric measurements, but at the same time low enough to be exempt from the regulatory control, as well as to avoid significant self-shielding.

The samples are either placed in locations which directly lie on key neutron streaming paths or in representative locations in rooms. They are attached to fixtures (such as pipes or handles) using an aluminum chain. The use of the more common steel chains is undesirable, due to neutron activation (since steel always contains cobalt impurities, producing ^{60}Co), which would necessitate the disposal of the chain as radioactive waste. In locations where only very low thermal flux is expected, the silver foil is omitted from the samples.

In order to compare the MCNP model simulation results with the foil measurements, the MCNP model is used to determine the reaction rates for the corresponding foil activation reactions. The variance reduction code ADVANTG [3] is used to accelerate these calculations. The calculated reaction rates are then combined with known cycle parameters (such as average power and cycle length) to determine the final activity of each corresponding foil. The agreement between the two is expressed as a ratio between the *calculated* and the *measured* value (C/M). Due to the small size of samples, substantial computational time is required for good statistics, given the large number of samples and the iterative nature of validation. Therefore, the Generic Sample Activation Model (GSAM) was developed [1]. Instead of implementing the small foils directly, a larger cell (typically a sphere of five centimeter diameter) is used to tally the neutron flux distribution. This result is then used to define the source in a simple MCNP model representing the sample inside the larger cell. This significantly reduces the computational time, albeit at the cost of introducing additional uncertainty, estimated to be in the order of 20% for a typical case [1].

3.2 Results

The C/M factors for all foils are shown in Figure 3, referring to the activities of the activation products of the three foils (^{60}Co, ^{110m}Ag, and ^{58}Co, respectively) plotted against the height (as indicated in Figure 1), since the axial trends dominate over radial and angular trends. The error bars are dominated by the aforementioned GSAM uncertainty (of approximately 20%), with reported activity measurement uncertainty typically around 2%.

The largest deviations occur in the bottom half of the drywell bulb (levels +1.0m, -2.7m, and -3.7m). Focusing on the C/M factors of the cobalt foils, as these are most representative of the neutron energy range leading to activation of cobalt and europium in concrete, we observe an overestimation of at least a factor of 2.5, which gradually increases with the decreasing height. At the height levels -2.72m and -3.72m the C/M factors range from 6.6 to 11.7, demonstrating a substantial overestimation in this area. The level -1.7m samples, corresponding to the control rod drive room, feature cobalt foil C/M factors between 2.5 and 3.6. For these sections, the deviations are primarily a result of the empty room assumption.

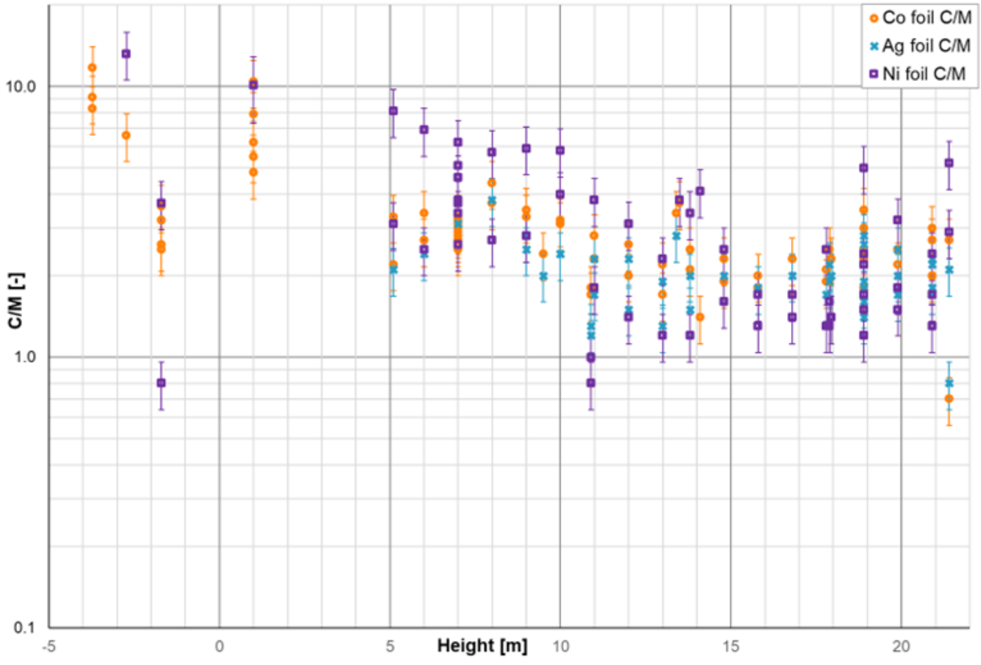

Figure 3. Flux Validation Results (C/M-values) plotted against reactor building height level.

4 Activation Validation through Gamma Spectrometry

The second technique used for the validation of AMAC models is based on the (mainly gamma, but sometimes also alpha and beta) spectrometry of the actual activated materials. For many components, such as the reactor internals, this can only be performed after the final shutdown of the plant, when the removal of material doesn't affect safety. However, limited sampling of the structures surrounding the RPV is possible even before the shutdown.

Three such campaigns are covered in this work. In August 2018, three samples were taken of the bioshield outer liner. Additionally, a 20-cm-long concrete drill core was extracted from the bioshield at +13.0m (just above the active core level) and divided into four equal sections. In August 2019, four drill cores were taken from the drywell wall at +16.6m, +14.7m, +11.8m, and +8.89, respectively. Following a detection of large overestimation at the lowest of these heights, a follow-up campaign was carried out in August 2020, extracting six drill cores at +9.6m, +9.4m, +4.3m, +4.2m, and (two cores at) +1.0m. The bioshield drill core is composed of baryte concrete, while all other drill cores are composed of normal concrete. No pieces of rebar reinforcement steel were detected in any of the drill cores. All drywell drill cores are shown in Figure 1, indicated by purple rectangles.

4.1 Methodology

Following the extraction, the drill cores were divided into smaller segments, with the range of depths corresponding to each segment recorded. These segments and the bioshield liner samples were then transferred to an on-site lab for gamma spectrometry evaluation.

Due to the high dose rate within the drywell, human access is limited. For this reason, only a few samples were extracted from the bioshield. Moreover, the drywell concrete drill cores were extracted from the outside of the drywell. Since none of the drill cores reached up to the inner liner of the drywell, this represents a potential source of uncertainty for the exact depth determination (being based on the outer drywell surface coordinates).

4.2 Results

The C/M factors for the aforementioned activation validation measurements are shown in Table 1 (for the bioshield) and Table 2 (for the drywell), respectively.

The uncertainties (not indicated in the tables) are primarily composed of the measurement uncertainties (in the order of 20%) and the calculation uncertainties—composed of uncertainties in location, impurity concentration, resolution of the energy group structure for activation calculations, and MCNP statistical uncertainty, altogether estimated to be in the order of 10%.

The C/M factors for the three samples of the bioshield liner show a significant variation, with the +17.8m sample being strongly overestimated and the other two samples being underestimated. These results also vary from the adjacent flux sample results. This variation in the bioshield liner sample results could be a product of variable cobalt impurity in the liner steel. Alternatively, it may be caused by the presence of shielding structures in the vicinity of the sample locations, which are not included in the MCNP model. However, due to the small overall number of bioshield liner samples, it is difficult to draw a general conclusion.

The concrete drill cores in the upper sections of the drywell (above the bulb) show a generally good agreement. The largest overestimation is again found in the drywell bulb section (as it was for the flux samples), and it grows with the decreasing height.

Table 1. Bioshield Activation Validation Results.

Bioshield liner

Height [m]	C/M ^{60}Co
7.1	0.5
13	0.5
17.8	19.3

Bioshield drill core 3, +13.0m

Depth [cm]	C/M		
	^{60}Co	^{152}Eu	^{133}Ba
0-5	1.3	1.8	1.2
5-10	1.6	2.0	1.3
10-15	2.6	3.5	1.8
15-20	2.7	3.3	1.4

Table 2. Drywell Activation Validation Results.

Drill core 4, +16.6m

Depth [cm]	C/M	
	^{60}Co	^{152}Eu
20.0	1.2	1.1
22.3	1.3	1.1
24.6	0.7	0.9
26.9	1.2	0.9
29.2	1.0	0.9
31.5	1.2	0.6
33.8	1.1	0.8
36.1	1.3	N/A
38.4	0.7	0.9
40.7	N/A	N/A
43.0	N/A	N/A
45.3	0.6	N/A

Drill core 3, +14.7m

Depth [cm]	C/M	
	^{60}Co	^{152}Eu
21.5	0.4	0.5
23.8	0.7	0.6
26.1	0.9	0.8
28.4	0.7	0.7
30.7	1.1	1.0
33.0	0.7	0.7
35.3	0.8	0.8
37.6	1.0	0.8
39.9	1.0	0.9
42.2	0.8	0.8
44.5	0.6	N/A
46.8	0.8	N/A
49.1	1.0	N/A

Drill core 2, +11.8m

Depth [cm]	C/M	
	^{60}Co	^{152}Eu
26.0	1.2	0.8
28.3	1.1	0.8
30.6	1.0	1.0
32.9	1.2	0.9
35.2	0.9	0.7
37.5	1.0	1.0
39.8	1.3	1.0
42.1	1.2	1.0
44.4	0.9	0.7
46.7	0.8	0.7
49.0	0.6	0.6
51.3	1.2	N/A
53.6	0.7	N/A

Drill core 11, +9.6m

Depth [cm]	C/M	
	^{152}Eu	^{60}Co
42.2	10.0	10.4
44.9	17.4	16.0
47.6	16.0	10.3
50.3	13.3	12.0
53.0	23.0	22.9
55.7	14.9	17.4
58.4	20.2	19.5
61.1	26.8	30.3
63.8	23.4	14.7
66.5	39.1	N/A
69.2	22.0	16.4
71.9	42.1	N/A
74.6	18.7	N/A

Drill core 12, +9.4m

Depth [cm]	C/M	
	^{152}Eu	^{60}Co
62.2	2.5	2.4
64.9	2.3	2.0
67.6	3.2	3.1
70.3	3.7	2.9
73.0	4.6	3.3
75.7	4.4	4.0
78.4	4.0	4.2
81.1	3.1	2.3
83.8	2.5	1.4
86.5	1.9	1.3
89.2	1.5	1.0
91.9	2.0	1.9
94.6	3.9	1.1
97.3	1.9	1.9
100.0	0.4	0.2

Drill core 1, +8.9m

Depth [cm]	C/M	
	^{60}Co	^{152}Eu
13.0	10.6	8.1
15.3	11.2	7.5
17.6	7.7	6.4
19.9	12.0	10.1
22.2	18.2	10.8
24.5	7.6	10.2
26.8	22.1	18.5
29.1	25.4	N/A
31.4	19.3	N/A

Table 2. Drywell Activation Validation Results (cont.)

Drill core 6, +4.3m

Depth [cm]	C/M	
	^{152}Eu	^{60}Co
12.2	13.9	16.3
14.9	11.6	13.2
17.6	11.4	10.0
20.3	10.8	11.9
23.0	8.5	7.2
25.7	9.9	11.2
28.4	8.6	6.6
31.1	11.8	7.3
33.8	15.6	N/A
36.5	24.0	N/A
39.2	11.2	N/A

Drill core 10, +4.2m

Depth [cm]	C/M	
	^{152}Eu	^{60}Co
10.2	6.0	7.1
12.9	5.0	9.2
15.6	9.1	5.9
18.3	2.3	8.6
21.0	8.4	7.5
23.7	7.0	8.4
26.4	9.5	10.9
29.1	8.6	N/A

Drill core 9, +1.0m

Depth [cm]	C/M	
	^{152}Eu	^{60}Co
6.2	23.6	17.9
8.9	23.6	20.8
11.6	19.8	22.7
14.3	14.2	10.7
17.0	19.3	13.5
19.7	13.4	7.1
22.4	7.9	7.4
25.1	5.0	5.2

Drill core 8, +1.0m

Depth [cm]	C/M	
	^{152}Eu	^{60}Co
10.2	12.3	16.8
12.9	14.9	13.6
15.6	14.8	17.0
18.3	13.2	8.3
21.0	13.4	13.1
23.7	12.8	N/A
26.4	16.2	N/A
29.1	11.7	11.1
31.8	24.0	N/A

5 Conclusion

In this work, the basis for a comprehensive validation of the KKM AMAC model simulation was presented, describing the results of two foil activation campaigns and three radiological measurement campaigns. The neutron flux and activation levels are found to be generally overestimated by the simulation, especially in the bottom half of the drywell bulb. These comparisons provide a first insight into the model's ability to predict neutron activation in the different regions of the KKM reactor building.

The future work will focus on uncertainty quantification, with a focus on the omitted room-filling structures (especially if shielding the validation samples from neutron radiation). Afterwards, the validation results will be used to define region-dependent scaling factors and thus enable the best estimate prediction of neutron activation for decommission planning.

The authors would like to acknowledge the support of Gerwin Spölgen (of BKW) and his contributions to organizing the KKM activation measurement campaigns.

References

1. V. Bykov, *High-Fidelity Determination of Nuclide Inventories for Radioactive Waste Disposal*, EPFL PhD Thesis (2019). DOI: 10.5075/epfl-thesis-8960.
2. C.J. Werner (editor), *MCNP Users Manual - Code Version 6.2*, LANL report LA-UR-17-29981 (2017).
3. S.W. Mosher et al. ADVANTG—An Automated Variance Reduction Parameter Generator. ORNL report TM-2013/416 (2021).